tal uncertainties, in this direction. We ascribe such a fact to be due to the low atomic concentration of the impurity, i.e., about 0.2 at.% in the melted thickness.

As to Cu-doped samples, we observed a very fine-grained structure with a change in the lattice constant. The presence of a crystalline structure could be explained in terms of a decrease in viscosity of pure aluminum due to the small addition of Cu impurity atoms (in our experiment the Cu concentration in the examined thickness is about 0.5 in atomic percent). Such a behavior is similar to the one observed in other metals doped with suitable metallic atoms.[11]

The increase in the lattice parameter may perhaps herald a situation very near to the crystal/glass transition. Such a transition is characterized by a volume expansion.[12] This effect is probably present in all our irradiated samples, but it is more easily detected in this case because of the crystallinity of the specimen.

Finally a transition from the amorphous to the crystalline phase was observed after annealing in vacuum at 400 °C for 30 min. Such a preliminary result obviously gives only an upper limit of the recrystallization temperature. We want to point out that the recrystallization temperature cannot be expected to coincide with some values found in annealing experiments of various defects in Al crystals; an amorphous state is not simply comparable with a crystal containing some defects. More detailed investigations are in progress to determine the crystallization behavior of the noncrystalline films we obtained.

[1]C. V. Gokularathnam, J. Mater. Sci. 9, 673 (1974).
[2]G. S. Cargill, III, in *Solid State Physics*, edited by F. Seitz, D. Turnbull, and H. Ehrenreich (Academic, New York, 1975), Vol. 30, p. 227.
[3]S. Takayama, J. Mater. Sci. 11, 164 (1976).
[4]Y. Waseda, H. Okazaki, and T. Masumoto, J. Mater. Sci. 12, 1927 (1977).
[5]K. Suzuki, in *Proceedings of the Symposium on Structure and Properties of Amorphous Metals, Iizaka, Fukushima, Japan, 9–11 December 1977*, edited by T. Masumoto and K. Suzuki (Sendai Kei, Sendai, Japan, 1978), p. 1.
[6]H. A. Davies, in Proceedings of the Third International Conference on Rapidly Quenched Metals, University of Sussex, Brighton, 3–7 July 1978 (to be published), Sect. A1.
[7]E. M. Breinan, B. H. Kear, and C. Banas, Phys. Today 29, No. 11, 44 (1976).
[8]S. C. Hsu, S. Chakravorty, and R. Mehrabian, Metall. Trans. 9B, 221 (1978).
[9]R. Tsu, R. T. Hodgson, T. Y. Tan, and J. E. Baglin, Phys. Rev. Lett. 42, 1356 (1979); P. L. Liu, R. Yen, N. Bloembergen, and R. T. Hodgson, Appl. Phys. Lett. 34, 864 (1979).
[10]G. Della Mea, L. Donà dalle Rose, P. Mazzoldi, and A. Miotello, Radiat. Eff. (to be published).
[11]A. R. Ubbelohde, *The Molten State of Matter* (Wiley, New York, 1978), p. 366.
[12]H. A. Davies and J. B. Hull, J. Mater. Sci. 11, 215 (1976).

Intensity of Plasmon Satellites in Ultrasoft-X-Ray Photoemission Spectra

Denis Chastenet
Laboratoire de Chimie-Physique, Université de Paris VI, F-75231 Paris, France

and

Pierre Longe
Institut de Physique B5, Université de Liège, Sart-Tilman, B-4000 Liège, Belgium

(Received 4 June 1979)

A calculation of the bulk-plasmon-satellite strengths in the photoemission spectra of metals is presented for the dispersionless plasmon model. The calculation is made for all energies, especially for the ultrasoft-x-ray regime. In this spectral region, the interference term between extrinsic and intrinsic plasmon productions is of the same order as the intrinsic production term. The photoelectron energy for which these two terms cancel each other exactly is determined.

Recently there has been a considerable interest in the observation of photoemission spectra (XPS) of metals in the *ultrasoft*-x-ray regime.[1-4] When the exciting photon energy is low enough so that the outgoing photoelectrons have an energy ϵ_k of a few times the plasmon energy ω_p, there is an important weakening of the plasmon satellite intensity due to a quantum interference term between extrinsic and intrinsic plasmon production.[5] Plasmons may indeed be excited either in

an extrinsic process by the photoelectron on its way out of the metal or in an intrinsic process by the core hole potential created at the moment of the x-ray absorption. The interference becomes particularly important for a slow photoelectron when both processes tend to occur in the same region, in the neighborhood of the x-ray absorption site. For these energies the situation tends to be similar to the one encountered in x-ray emission or absorption spectra[6] where the plasmon satellite is very weak (a few percent of the main band intensity).

In the present paper this important interference effect is calculated for the first time for arbitrary photoelectron energy, using a nonperturbative treatment. Some years ago Chang and Langreth (CL)[7] calculated this effect in a lowest-order perturbative expansion for high energies ($\epsilon_k > 300$ eV). In their calculation the expansion parameter is $(R_\infty/\epsilon_k)^{1/2}$. The metal fills the half-space $z<0$ and is represented by the jellium model, the only parameter being the electron-density parameter r_s. Also the surface modes are disregarded and the only energy losses are due to the excitation of bulk plasmons which are assumed to be undamped and dispersionless, with wave vectors $q \leq q_c$. Using this model CL calculate the strengths of the successive plasmon satellites, which are related to the areas of the observed peaks (integrated intensities). They thus disregard the detailed line shape which manifests tailing effects due to plasmon dispersion and continuous energy losses (electron-hole pairs). According to CL, the strength of the nth satellite is given by

$$e^{-\beta'} \sum_{\mu=0}^{n} \frac{\beta'^{\mu}}{\mu!}, \tag{1}$$

where

$$\beta' = \beta - (R_\infty/\epsilon_k)^{1/2} F(\epsilon_k) \tag{2}$$

and

$$\beta = e^2 g_c/\pi\omega_p . \tag{3}$$

Expression (1) was first proposed by Langreth[8] with $\beta' = \beta$ where β, previously calculated by Lundqvist,[9] is essentially related to the intrinsic plasmon production and is independent of ϵ_k. Then CL introduced β' given by (2) where the second, negative term describes the interference effect. Note that when $\beta' = 0$, one has a pure extrinsic spectra where according to (1) all the satellites and the main peak ($n = 0$) have the same strength (equal to 1) in agreement with a Poisson-like analysis. However, the CL theory, where $F(\epsilon_k)$ is expanded perturbatively about $F(\infty) = \frac{1}{2}\pi$, is clearly invalid at low energies, since β' cannot be negative. In the present paper we present an accurate treatment of the plasmon-satellite strength, using the above jellium model, but calculating $F(\epsilon_k)$ for all energies and introducing an electron mean free path depending on ϵ_k. We also provide below a set of equations [Eqs. (5), (9), (10), and (7)], which can be extended to more varied and realistic situations than the semi-infinite jellium, for instance thin films, depth-dependent ionization or electron density, nonorthogonal emission, surface structures, etc.

In contrast with CL or other previous analyses[10] where the photoelectron is a recoilless classical particle coupled to plasmon modes, we start from an S- and T-matrix approach and a requirement of conservation of probability. Such an approach yields a *unified* method to calculate the intrinsic and extrinsic terms for all energies.

The calculations being rather short, we shall present them in some detail with a view to possible extensions by the reader to other geometrical or physical situations. The strength of the nth peak, related to the excitation of n plasmons, can be written in the usual form:

$$I_n(\epsilon_k) = \int_{-\infty}^{0} dz\, \rho(z) J_n(\epsilon_k, z), \tag{4}$$

where $J_n(\epsilon_k, z)$ is the probability that a photoelectron has a path of length z across the metal and leaves the surface with kinetic energy ϵ_k; $\rho(z)$ is the primary ionization density. However, instead of dealing with parameter z, we shall introduce the transit time $\tau = z/v_k$ as our basic parameter (v_k is the electron velocity along the path) and we write

$$I_n(\epsilon_k) = \int_{-\infty}^{0} d\tau\, v_k \rho(\tau) J_n(\epsilon_k, \tau) \tag{5}$$

where ρ is a constant (equal to 1) in the present model. The production rate $J_n(\epsilon_k, z)$ is related to the S-matrix element by the golden rule

$$J_n(\epsilon_k, \tau) = (n!/2\pi N t_0) \int d^3q_1 \cdots \int d^3q_n |S_n(\tau, \epsilon_k)|^2, \tag{6}$$

the $\vec{q}$'s being the external plasmon momenta and t_0 the observation time. The normalization fac-

tor $1/N$ is determined by the sum rule

$$\int_{\epsilon_F}^{\omega+\epsilon_B} d\epsilon_k \sum_{n=0}^{\infty} J_n(\tau, \epsilon_k) = 1, \tag{7}$$

which is required by the condition of conservation of photoelectron number.

A typical diagram describing the matrix element $S_n(\tau, \epsilon_k)$ is given in Fig. 1 (for $n=3$). Extrinsic plasmons are attached to the upward photoelectron line, intrinsic plasmons to the downward core-hole line. All the extrinsic plasmon vertices appear on the photoelectron is created, and time $t+\tau$ when it reaches the metal surface represented by the black dot.

Let us first consider only the external plasmon lines in Fig. 1. The S-matrix element related to nth satellite takes the form

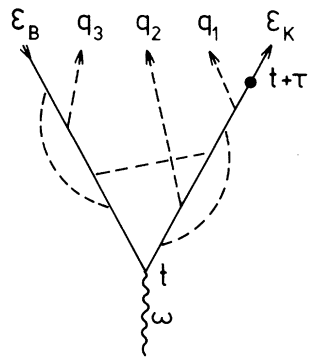

FIG. 1. Example of photoemission diagram with extrinsic (q_1 and q_2) and intrinsic (q_3) plasma production.

$$S_n(\epsilon_k) = \frac{1}{i}\int dt\, g(t) \exp[i(\epsilon_k + n\omega_p - \epsilon_B - \omega)t] \frac{1}{n!} \prod_{\mu=0}^{n} \left[\frac{1}{i} \frac{\omega_p V(q_\mu)}{2(2\pi)^3}^{1/2} \left(\frac{1}{\omega_p} - \frac{1 - i\exp[i\nu(\vec{k}, \vec{q}_\mu)\tau]}{\nu(\vec{k}, \vec{q}_\mu)}\right)\right] \tag{8}$$

with

$$\nu(\vec{k}, \vec{q}) = \omega + \epsilon_k - \epsilon_{|\vec{k}+\vec{q}|}.$$

Potential $V(q)$ is the bare Coulomb potential and $g(t)$ an adiabatic function stationary for a time t_0.[11]

Substitution of (8) into (6) gives

$$J_n(\tau, \epsilon_k) = \delta(\epsilon_k + n\omega_p - \omega - \epsilon_B) T(\tau, \epsilon_k)^n (Nn!), \tag{9}$$

where the T-matrix element has the form

$$T(\tau, \epsilon_k) = \frac{\omega_p}{2(2\pi)^3} \int d^3q\, V(q) \left| \frac{1}{\omega_p} - \frac{1 - \exp[i\nu(\vec{k}, \vec{q}_\mu)\tau]}{\nu(\vec{k}, \vec{q}_\mu)} \right|^2. \tag{10}$$

Expression (8) involves an approximation. The same energy ϵ_k appears in all the photoelectron propagators $1/\nu(\vec{k}, \vec{q})$. This means that the energy is not conserved along the photoelectron line. This approximation is sensible, however. The calculation remains exact for the main peak ($n=0$) and first satellite ($n=1$), and the momentum is conserved at all vertices, as opposed to what has been done in previous papers.[7-10] Moreover, for the small-k limit, (10) is in agreement with the former theories on x-ray spectra,[6] which give a very good description of the observed weak satellite. These theories are based on equations similar to (9) and (10) where the term $-\exp(i\nu t)$ has been dropped (infinite τ).

To introduce the effect of the internal plasmon lines we proceed to a vertex renormalization by calculating N from the sum rule (7). Such a method, consistent with the above approximation, yields an expression for N which depends on τ. Note that N would be a constant if the internal plasmon line were explicitly introduced in the S_n's.

The basic equations of our theory are thus (5), (9), (10), and (7). Let us apply them to the semi-infinite jellium, where we can assume $\tau \gg \omega_p^{-1}$.[12] The T-matrix element becomes

$$T(\tau, \epsilon_k) = \beta - \left(\frac{R_\infty}{\epsilon_k}\right)^{1/2} F(\epsilon_k) + \Gamma(\epsilon_k)\tau, \tag{11}$$

where

$$\Gamma(\epsilon_k) = me^2\omega_p k^{-1} \ln b$$

and

$$F(\epsilon_k) = \frac{1}{\pi}\int_a^b \frac{dx}{x} \ln\left|\frac{x+1}{x-1}\right| = \frac{\pi}{2} - \frac{2}{\pi} \sum_{s\,(\text{odd})}^{\infty} \frac{a^s + b^{-s}}{s^2}$$

with a (or b) $= q_c[(k^2 + 2m\omega_p)^{1/2} \pm k]^{-1}$. We then proceed to the calculation of N and the I_n's along the above lines. Note that for large ϵ_k, we have

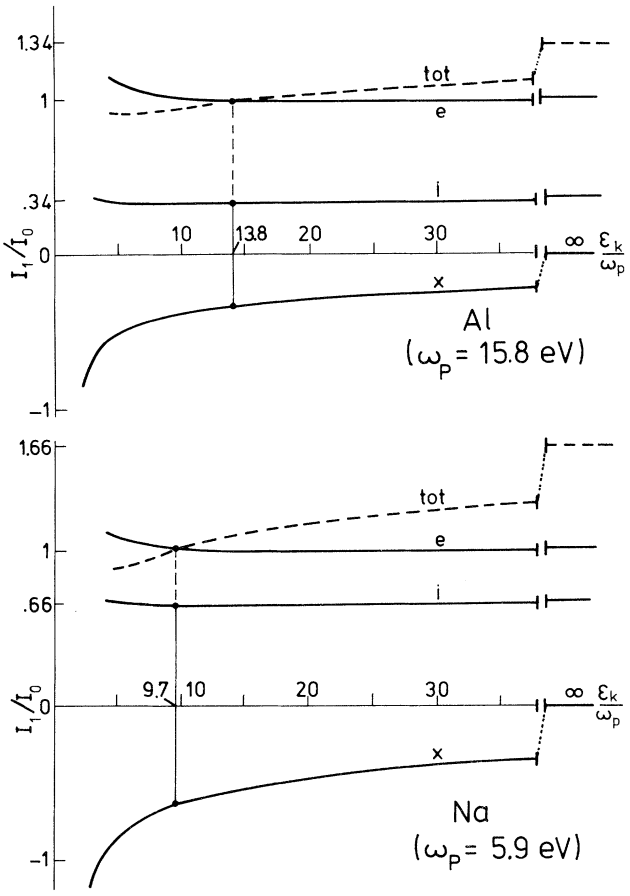

FIG. 2. Contributions to the intensity ratio I_1/I_0 between the first satellite and the main line, related to extrinsic and intrinsic plasmon production (curves *e* and *i*) and to the interference term (curves *x*). The total ratio I_1/I_0 is represented by the dashed curve. For high energies these three terms *e*, *i*, and *x* tend, respectively, to 1, to β (0.34 for Al and 0.66 for Na), and to $(\frac{1}{2}\pi)(R_\infty/\epsilon_k)^{1/2} \sim 0$.

the following limits: $\Gamma(\epsilon_k)$ tends to the usual electron damping expression, $F(\epsilon_k)$ to the CL upper limit $F(\infty) = \frac{1}{2}\pi$, and N to the form $\exp[T(\tau, \epsilon_k)]$, and finally the J_n's given by (9) tend to Poisson-like expressions. The important point, however, is that here our I_n's are valid for all energies.

Figure 2 gives the three contributions to the ratio I_1/I_0 coming from the intrinsic and extrinsic plasmon productions and their interference term. This negative interference term is thus the only one which strongly depends on ϵ_k. Figure 2 also shows the energy for which the interference term cancels the intrinsic term.[13] In the case of Al this occurs for $\epsilon_k = \omega + \epsilon_B - \omega_p = 13.8\omega_p = 218$ eV, and in the case of Na for $\epsilon_k = 9.7\omega_p = 57$ eV. For these energies the photoemission spectra should be similar to the energy-loss spectra generated by transmission of electrons through metals.

In a very recent paper,[4] Johansson and Lindau have emphasized a discrepancy between the observed ratio I_1/I_0 for Al and the same ratio yielded by a purely extrinsic theory. This discrepancy can be estimated as varying from 0 to 0.3 in a spectral region extending from 200 to 40 eV (i.e., between $13\omega_p$ and $3\omega_p$). It is thus of the same order as the deviation appearing in Fig. 2 between the dashed (total) curve and the extrinsic (*e*) curve. Such a result is encouraging, the actual problem being an adequate estimation of the areas of the peaks and of the background from the theoretical[14] as well as from the experimental point of view.

We are grateful to C. Bonnelle and S. M. Bose for useful discussions. This work was supported in part by the Centre National de la Researche Scientifique, France, and in part by the Fonds National de la Recherche Scientifique, Belgium.

[1]S. A. Flodstrom, R. Z. Bachrach, R. S. Bauer, J. C. McMenamin, and S. B. M. Hagström, J. Vac. Sci. Technol. 14, 303 (1977).

[2]R. S. Williams, P. S. Wehner, G. Apai, J. Stöhr, D. A. Shirley, and S. P. Kowalczyk, J. Electron Spectrosc. Relat. Phenom. 12, 477 (1977).

[3]D. Norman and D. P. Woodruff, Surf. Sci. 79, 76 (1979).

[4]L. I. Johansson and I. Lindau, Solid State Commun. 29, 379 (1979).

[5]For a review of the field see J. W. Gadzuk, in *Photoemission and The Electronic Properties of Surfaces*, edited by B. Feuerbacher, B. Fitton, and R. F. Willis (Wiley-Interscience, New York, 1978), p. 111.

[6]A. J. Glick and P. Longe, Phys. Rev. Lett. 15, 589 (1965); F. Brouers and P. Longe, in *Soft X-Ray Band Spectra*, edited by D. J. Fabian (Academic, London, 1968), p. 329; B. Bergersen, F. Brouers, and P. Longe, J. Phys. F 1, 945 (1971).

[7]J. C. Chang and D. C. Langreth, Phys. Rev. B 5, 3512 (1972); D. C. Langreth, in *Collective Properties of Physical Systems*, 24th Nobel Symposium, edited by B. I. Lundqvist and S. Lundqvist (Academic, New York, 1974), p. 210.

[8]D. C. Langreth, Phys. Rev. B 1, 471 (1970).

[9]B. I. Lundqvist, Phys. Kondens. Mater. 9, 236 (1969).

[10]M. Šunjić, D. Šokčević, and A. A. Lucas, J. Electron Spectrosc. Relat. Phenom. 5, 963 (1974); M. Šunjić and D. Šokčević, Solid State Commun. 15, 165 (1974), and 18, 373 (1976).

[11]L. I. Schiff, *Quantum Mechanics* (McGraw-Hill, New York, 1968), 3rd ed., p. 312.

[12]When thin films or surface structures are considered,

(10) has to be kept.

[13]In some recent papers, the interference effect and its strong energy dependence seem to be underestimated in spite of the CL theory. See, e. g., W. J. Pardee, G. D. Mahan, D. E. Eastman, R. A. Pollak, L. Ley, F. R. McFeely, S. P. Kowalczyk, and D. A. Shirley, Phys. Rev. B 11, 3614 (1975), and D. R. Penn, Phys. Rev. Lett. 38, 1429 (1977), where the role of intrinsic versus extrinsic plasmon production is discussed, but where the experimental data do not mention the photoelectron or exciting radiation energy.

[14]S. M. Bose, P. Kiehm, and P. Longe, to be published.

Experimental Exchange-Split Energy-Band Dispersions for Fe, Co, and Ni

D. E. Eastman, F. J. Himpsel, and J. A. Knapp
IBM Thomas J. Watson Research Center, Yorktown Heights, New York 10598
(Received 24 July 1979)

Using angle-resolved photoemission with single-crystal Fe(111) and Co(0001), we have determined accurate exchange-split energy-band dispersions $E(\vec{k})$ along symmetry lines. For Fe, Co, and Ni, respectively, occupied d-band widths are 3.1 eV (P), 3.8 eV (L), and 3.4 eV (L,X) while exchange splittings are ~ 1.5 eV (P), ~ 1.1 eV (Γ), and 0.3 eV (near L). Comparison with theory shows that state-of-the-art *ab initio* calculations describe the strong ferromagnets Fe and Co much better than Ni.

A long-standing goal has been the determination of accurate exchange-split energy-band dispersions for the itinerant-electron ferromagnets Fe, Co, and Ni.[1-14] As often noted,[2,4] magnetic exchange splittings and energy-band dispersions $E(\vec{k})$ are fundamental for understanding various physical properties involving d-band electronic structure,[1-4] collective itinerant-electron ferromagnetism,[5,6] transition-metal surfaces, etc. Recently, the temperature-dependent exchange splitting and energy-band dispersions for Ni have been determined.[13,14] For Fe and Co, however, exchange splittings and energy-band dispersions remain inconclusive or absent despite several angle-resolved photoemission studies[9-12] and other ultraviolet and x-ray photoemission studies.[7,8] Rather, contradictory conclusions have been reached, i.e., (i) that angle-resolved photoemission spectra measure a density of states[12] [nondirect-transition model, in which case $E(\vec{k})$ dispersions cannot be determined] and (ii) that direct transitions (with band dispersions[10]) are sometimes of primary importance but also more complicated effects, e.g., surface/polarization effects are sometimes predominant.[9-11]

In this paper, we show that direct transitions are of primary importance for normal photoemission from Fe(111) and Co(0001) and determine accurate exchange-split energy-band dispersions $E(\vec{k})$ for bcc Fe along the Γ–P–H symmetry line and for hcp Co along the Γ–A–Γ line. These results together with experimental $E(\vec{k})$ dispersions for Ni (Refs. 13 and 14) and Cu (Ref. 15) permit us to systematically compared with state-of-the-art *ab initio* band calculations.[1] This comparison shows that the ratio of the theoretical to experimental occupied d-band width is about 1.1, 1.2, 1.45, and 1.1 for Fe, Co, Ni, and Cu, respectively, while the ratio of the theoretical to experimental exchange splitting δE_{ex} is about 1.0, 1.2, and 2.2 for Fe, Co, and Ni, respectively. General conclusions are as follows: (1) Fe, Co, and Ni can all be described by a Stoner-Wohlfarth-Slater (SWS) spin-split energy-band model, and (2) state-of-the-art *ab initio* one-electron band calculations describe Fe quite well even though it has a large exchange splitting and high Curie temperature (strong ferromagnet), in marked contrast with Ni.

Experimentally, we have used a display-type electron spectrometer[14,15] and an ultrahigh-vacuum toroidal-grating monochromator together with radiation from the 240-MeV storage ring at the University of Wisconsin–Madison. This system was used for this study in the energy range $5 \leq h\nu \leq 30$ eV with an overall energy resolution of ~100–150 MeV and angular resolution of $\delta\theta = 4°$ (full angle). Fe(111), Fe(100), and Co(0001) crystals were prepared by Ar-ion etching and annealing, checked with use of Auger spectroscopy and low-energy electron diffraction, and measured in working vacuums in the 10^{-11}-Torr range.

In Fig. 1 we present selected angle-resolved energy distribution curves (AREDC's) for normal emission for Fe(111), Co(0001), and Ni(111). The pronounced spectral changes with photon energy $h\nu$ indicate that direct interband transitions are of primary importance. Consequently, these normal-emission spectra directly probe electron-